MODELLING OF URBAN CANYON: ANALYTICAL AND EXPERIMENTAL REMARKS

F.Rossi[1], F. Cotana[1], V. Coccia[*1], A.L. Pisello[1], E. Bonamente[1], M. Palombo[1], G. Pignatta[1], and E. Morini[1]

1 CIRIAF – Interuniversity Research Center on Pollution and Environment "M. Felli"
University of Perugia, Italy
Via G. Duranti, 06125, Perugia, Italy
**Corresponding author: e-mail coccia@crbnet.it*

ABSTRACT

The urban climate of high-density areas is often affected by an increase of the air temperature known as Urban Heat Island (UHI) phenomenon.
UHI is strongly influenced by the solar reflectance of conventional materials used for building envelope and urban coatings, i.e. streets and square pavings.
The present work proposes an original method to predict the temperature of both facades and local air mass on urban scenarios. The effect of changes on coatings may also be estimated.
The proposed method is based on an Experimental Facility (EF) and a Theoretical Model (TM) which are jointly taken into account for UHI predictions.
EF is located at the University of Perugia which is composed of two separate metal rails incorporating several insulating frames, resembling a urban canyon, positioned at different mutual height/distance ratios (i.e. H/D = 0.5, 1.0, 2.0). Each frame can be equipped with particular reflective films (e.g. cool roofs coatings) in order to assess variation of radiative exchanges as a function of geometry, meteorological conditions, and radiative properties of walls. The monitoring system is equipped with temperature sensors, a pyranometer and an anemometer. A weather station is located nearby.
EF may be used directly to estimate UHI by a mechanical analogy which however introduces strong limitation on real scenario dimensions and operative conditions.
By validating the TM via EF the range of real scenario may be studied and predicted is widely extended and the proposed method may be applied virtually for any case.
The preliminary calibration of the methodology using measured data is also presented.

KEYWORDS

Urban Heat Island effect, Urban canyon, Climate modelling, Building envelope, Cool roofs

1 INTRODUCTION

UHI is a well-known urban phenomenon which witnesses an increase of air temperature especially on summer time; the main consequences of UHI are an increase on building energy demand and a reduction of comfort condition [1]. Howard et al. [2] were the first who documented the temperature differences between an urban area and a rural one; this phenomenon was later named ''Urban Heat Island'' by Manley [3]. Although UHI related to winter time is not as much studued as for summer time, a few interesting contributions focused on the overall year-round have been issued, such as the work by Giridharan et al. [4], where a 9.0 °C difference between urban-rural conditions on winter time was registered.

The most relevant parameters impacting UHI are urban surfaces albedo, evapotranspiration and anthropogenic heating [5]. Many research contributions showed that an effective strategy to mitigate UHI consists of the implementation of high-reflective envelopes (e.g. cool roofs [6]) on behalf of conventional "darker" coatings [7]. Most of the research investigation on technologies to mitigate UHI were aimed to reduce energy

demand for cooling and GHG emissions.

At a local scale, UHI mitigation also improved the indoor thermal comfort of buildings [8]. The thermal behavior of a case-study scholar building in Athens was analysed through dynamic simulation modelling, showing a decrease in the annual cooling load of 40% after the installation of cool roofs. The same fundamental results were also experimentally documented by the same study and other scientists' contributions [9]. In fact, Kolokotsa et al. [10] showed that also the indoor thermal performance of non–conditioned buildings is influenced by UHI. This work concerning a university lab building located in Iraklion, Crete, demonstrated an year-round energy saving of 19.8%, and 27% for the summer period, achieved by applying cool roofs as a strategy to mitigate the urban temperature increase. Additionally, together with such inter-building effect [11], the potentialities of high-reflective irradiated surfaces have important impacts also on the global warming reduction. Akbari et al. [12] demonstrated that the increase in global average air temperature is directly linked to the reflectance capability of coatings exposed to solar radiation and located in urban areas.

A tool to estimate UHI and to test different material for coating would help researcher, administrators and low makers to better design urban ambient.

In this paper an original method to predict the temperature of both facades and local air mass on urban areas is proposed. By that the effect of changes on coatings is estimated which may be helpful for the energy design of a building. The proposed method is based on an Experimental Facility (EF) and a Theoretical Model (TM) which are jointly taken into account for UHI predictions. EF may be used directly to estimate UHI by a mechanical analogy which however introduces strong limitation on real scenario dimensions and operative conditions. By validating the TM via EF the range of real scenario may be studied and predicted is widely extended and the proposed method may be applied virtually for any case. Preliminary experimental data are presented.

1.1 Urban Canyon models

Numerical and analytical models can predict the spatial and temporal variation of UHI as a function of the relevant geometries of the urban context and reflectance features of building envelopes and urban coverings.

Gobakis et al. [13] applied neural-network techniques to the urban heat island modelling: the work showed the correlation between measured and predicted UHI parameters for several sites: the UHI intensity can be predicted quite accurately for at least a 24-h time horizon using a limited set of data.

The urban canyon effect was also modelled by Allegrini et al. in [14], by applying building dynamic simulation tools. Simulations were carried out for stand-alone buildings and buildings located in street canyons; the study showed the importance of accounting for the local urban microclimate when predicting the energy demands for buildings in urban areas. Geometry (i.e. aspect ratio) of urban canyons is also a key factor regulating the radiative flux exchange among different surfaces. With dynamic thermal simulations, Strømann-Andersen et al. [15] found that geometry variation is able to modify the overall energy consumption up to +30% for offices and +19% for housing. Also reflectivity features of the canyon surfaces play an important role in the thermal behavior of buildings. For instance, Doya et al. [16]

Figure 1: Panoramic view of the test field installation.

showed the positive effect of cool roofs against urban heat island, by monitoring a micro-scale experimental case study representing a typical urban canyon geometry. Additionally, the canyon geometry plays an important role also in terms of streets air quality. In fact, Chan et al. [17] showed that the pollutant transport and diffusion is influenced by the canyon aspect ratio.

The UHI can be influenced by the micro-climate conditions as well. In particular, with respect to the climate characterization, Krüger et al. [18] studied the impact of canopy geometry and building orientation on building cooling loads. Also the average wind speed is taken into account in the calculations and it was found that the highest increase in cooling loads is related to the highest urban concentration geometry. For particular cases, the simulation showed an increase in energy demand for cooling up to 250% and a decrease for winter heating up to 40%.

A urban heat storage model (UHSM) has been proposed by Bonacquisti et al. [19]. The authors used this urban canopy layer model to study the thermal anomalies between central Rome and its sub-urban surroundings. The validated results showed that the greatest difference between urban and rural temperatures is about 2°C during winter and 5°C during summer. As expected, such differences are directly related to the urban geometry and the optic-energy properties of materials.

The influence of the urban texture on building energy consumption was also studied by Ratti et al. [20] applying Digital Elevation Model (DEM). The surface-to-volume parameter was considered as representative to describe the urbanization rate of several cities such as London, Toulouse and Berlin. The work showed that the DEMs analysis could be used to explore the effects of the urban texture on the energy performance of buildings by taking into account the canyon geometry, the mutual shadowing, and window-to-wall ratios.

In this articulate research perspective, the model of the Urban Canyon as a function of its aspect ratio and radiative properties of its surfaces represents the focus of the work. The proposed analytic model is based on an energy-balance approach, and it takes into account the incoming solar radiation, the reflective properties of the canyon surfaces (both vertical walls and the ground surface), the convective heat transfer, and the characteristic height to distance ratio (H/D). As a result, the temperatures of the canyon surfaces can be estimated.

The present work proposes an original method to predict the temperature of both facades and local air mass on urban scenarios. The effect of changes on coatings may also be estimated.

The proposed method is based on an Experimental Facility (EF) and a Theoretical Model (TM) which are jointly taken into account for UHI predictions.

EF may be used directly to estimate UHI by a mechanical analogy which however introduces strong limitation on real scenario dimensions and operative conditions.

By validating the TM via EF the range of real scenario may be studied and predicted is widely extended and the proposed method may be applied virtually for any case.

The preliminary calibration of the methodology using measured data is also presented.

2 THE EXPERIMENTAL FACILITY (EF)

The EF is located on the roof of one the buildings at the University of Perugia, Italy (lat. 43° 6’ 44”N), as shown in Figure 1. It consists of two twin arrays, designed to monitor and compare the thermal behavior of two canyons featuring the same geometry and different reflective properties. Each test field is composed of four metal frames (0.6 m high, 4.2 m long) supporting insulating panels (0.2 m thick). The orientation of the frames, currently South-North, can be adjusted. The panel pitch can also be changed to reproduce different aspect ratios (H/W). In the presented configuration the investigated values of the aspect ratios are 0.5, 1.0 and 2.0 (Figure 2). A bituminous membrane was laid on the ground to resemble the radiative properties of the road surface. A total of 48 surface temperature sensors (i.e. type K thermocouples) were installed on the 16 sides: each side is instrumented with 2 sensors positioned along the vertical axis (to minimize boundary effects) at 0.2 and 0.4 m from the ground. The ground temperatures of each inner canyon, and open north- and south-facing canyons are also measured. Two sensors are used for each inner canyon (at 1/3 and 2/3 of the canyon width) and one sensor is used for each open canyon (0.4 m far from the vertical surface). One air temperature sensor is also positioned at the centre of each inner canyon (0.3 m high) and another one on each open canyon (0.3 m above the ground temperature sensor). An upward-facing pyranometer is also used. Continuous monitored data by a fully equipped meteorological station, positioned in the same experimental site are also available.

3 THE THEORETICAL MODEL (TM)

The TM proposed here is based on an energy-balance approach. The incoming solar energy enters the canyon and it is reflected or absorbed by the sun-exposed surface. It is supposed that no energy is transmitted through the ground nor through the vertical walls. When the

Figure 2: Close view of the West (in front) and East (behind) test fields before cabling. Each field is composed of 3 canyons with H/D ratios equal to 1.0, 0.5, and 2.0 (from left to right respectively).

radiant flux strikes a sun-exposed surface, part of it is diffusively reflected and part is absorbed as in the following equations:

$$R_{refl} = r \cdot R_{sun}$$
$$R_{abs} = a \cdot R_{sun}$$

$$r + a = 1 \quad (1)$$

where R_{sun} is the incoming solar radiation normal to the surface, R_{refl} and R_{abs} the reflected and absorbed radiations, respectively. The reflection (r) and absorption (a) coefficients in eq. (1) are associated to the visible portion of the electromagnetic spectrum, and, more precisely, they have to be interpreted as solar reflection and absorption indices [21-22]. As in the common real case, the reflection is considered to be diffused. According to the proper view factor, the reflected light can escape from above and/or strike another surface of the canyon (e.g. a shadowed wall or the ground) where part of it is absorbed and part is reflected again. This process is iterated until all the visible light is either absorbed or exits the canyon. At each step the absorbed energy produces an increase of the surface temperature (T), and it is re-emitted according to:

$$G = \epsilon \cdot \sigma_0 \cdot T^4 \quad (2)$$

being ϵ the surface emissivity and σ_0 the Stefan-Boltzmann constant. For temperatures close to the standard ambient conditions the radiation is emitted at infrared wavelengths. Infrared radiation undergoes a multiple reflection/absorption/reemission process, similar to that of visible light but characterized by infrared absorption (α) and reflection (ρ) coefficients. As for the visible spectrum it is assumed that there is no transmitted infrared radiation:

$$\rho = 1 - \alpha, \ \alpha = \epsilon \quad (3)$$

The canyon is modelled as a parallelepiped. It is delimited by 6 surfaces: the ground, the sun-exposed and shadowed surfaces, the sides and the top of the canyon (

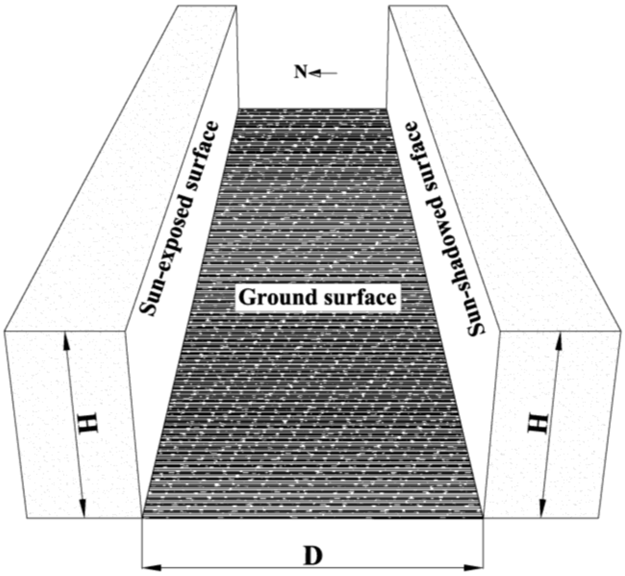

Figure **3**). These last three surfaces are opened and solar radiation (both visible and infrared) can exit the canyon through them.

The canyon is parameterized by three linear dimensions: length (hereafter referred to as L), height (H) and distance (D). Changing their values, it is possible to produce differently shaped canyons, spanning over all possible aspect rations (H/D) and enhancing or dimming side-effects (depending on L).
For a given geometry, an energy balance is run considering the total energy reaching and leaving each surface. Three sets of equations are used: one for the visible radiation, one for the infrared radiation, and one for the overall energy balance, including convection.
The visible radiosity (R) is defined as the radiant visible flux (W/m^2) leaving a surface. It is given by:

$$R_i . S_i = r_i \cdot \sum_{j \neq i} R_j \cdot S_j \cdot F_{j \rightarrow i} + R_{sun,i} \cdot S_i \quad (4)$$

where $S_{i(j)}$ is the extension of surface *i(j)*, r_i is the visible reflection coefficient, and $F_{j \rightarrow i}$ is the view factor from surface *j* to surface *i*. $R_{sun,i}$ is the normal component of the solar flux on the surface *i*

$$R_{sun,i} = R_{sun} \cdot cos\ \theta \quad (5)$$

where θ, the angle between the normal to the surface and the sun beam, is a function of the solar altitude (β) and azimuth (φ) angles, and the orientation and inclination of the surface itself. $R_{sun,i}$ is zero for a shadowed surface.
The infrared radiosity (*G*), defined similarly to *R*, includes the thermal flux radiated from the surface:

$$G_i . S_i = \alpha_i \cdot \sigma_0 \cdot T_i^4 \cdot S_i + \rho_i \cdot \sum_{j \neq i} G_j \cdot S_j \cdot F_{j \rightarrow i} \quad (6)$$

The global energy balance on each surface is defined by the following equation:

$$R_{sun,i} \cdot S_i + \sum_{j \neq i} (R_j + G_j) \cdot S_j \cdot F_{j \rightarrow i} = (R_i + G_i) \cdot S_i + h_i^c \cdot (T_i - T_{in}) \cdot S_i \quad (7)$$

where $h^c{}_i$ is the heat transfer coefficient of surface *i* and T_{in} is the air temperature inside the canyon. The convection coefficient $h^c{}_i$ can be directly computed from the surface and air properties, and the system geometry.
A final equation defines the energy balance on the top open surface (S_{sky}):

$$\sum_i R_{sun,i} \cdot S_i = \sum_{j \neq sky} (R_j + G_j) \cdot S_j \cdot F_{j \rightarrow sky} \quad (8)$$

where *i* marks the sun-exposed surfaces, *j* marks all the canyon surfaces, and $F_{j \rightarrow sky}$ is the

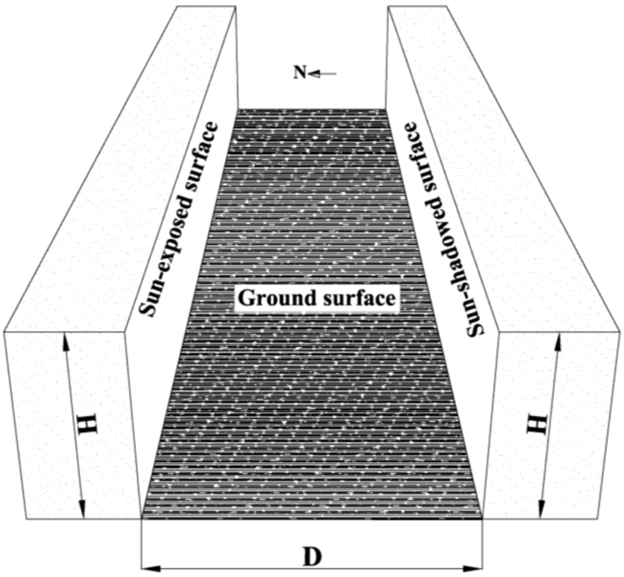

Figure **3:** Sketch of the urban canyon geometry parameters. The aspect ratio is defined by the ration of the height (H) over the distance (D).

view factor form surface *j* to the top surface (i.e. the sky).
The TM is defined by a total of 10 equations, 3 for visible radiosities (eq. (4)), 3 for infrared radiosities (eq. (6)), 3 for the total energy on the canyon surfaces (eq. (7)), and 1 for energy through the top surface (eq. (8)). The system is fully determined, having a total of 10 unknown variables R_1, R_2, R_3, G_1, G_2, G_3, T_1, T_2, T_3, and T_{in}, where subscripts from 1 to 3 mark the canyon inside surfaces and T_{in} is the inside air temperature.

Two different scenarios can be reproduced for the convective heat exchange, one for dominant natural convection and one for dominant forced convection.

Natural convection

In the case of natural convection, h_c is given by:

$$hc = Nu \cdot \frac{\lambda}{l} \tag{9}$$

$$Nu = c_{h,v} \cdot Ra^{1/3} \tag{10}$$

$$Ra = \frac{a \cdot g \cdot \theta \cdot l^3 \cdot \rho^2 \cdot \gamma}{\mu \cdot \lambda} \tag{11}$$

where Nu is the Nusselt number, $c_{h,v}$ a constant taking different values for horizontal and vertical surfaces, and Ra the Rayleigh number [23].
Since in eq. (11) the term $A = \frac{(a \cdot g \cdot \rho^2 \cdot \gamma)}{\mu \cdot \lambda}$ is only dependent on the specific properties of the fluid participating in the convective heat transfer, it is univocally calculated. Therefore, the Rayleigh number can be written as

$$Ra = A \cdot \theta \cdot L^3 \tag{12}$$

A mechanical analogy (i.e. similitude approach) is needed to relate the experimental data found on the EF to a real-size scenario. The same convective exchange is guaranteed if the two systems have the same the Rayleigh number:

$$\mathrm{Ra} = \mathrm{Ra_M} \tag{13}$$
$$\theta \cdot L^3 = \theta_M \cdot L_M^3 \tag{14}$$

In the case of a EF with a characteristic length L_M, the above condition can be achieved forcing an appropriate θ_M. Changing the EF parameters, different real scenarios, characterized by L and θ, can be reproduced. For example, forcing θ_M=55°C and using typical real-condition values θ=5°C, a scale factor of $L_M/L \approx 0.3$ is achieved:

$$L_M = \sqrt[3]{\frac{\theta}{\theta_M}} \cdot L \tag{15}$$

An alternative, hard to carry out, solution is represented by the replacement of the fluid (i.e. the A parameter of eq. 12).
The condition given by eq. (15) may be achieved making adjustments on the EF, that are:

- to use a protection barrier from the external wind without modifying the insolation conditions;
- to install adjustable warming plates on EF pavement.

In addition, the next configuration of the EF will include a rotating platform to follow the Sun-path. Figure 4 shows the configuration of the EF for the natural convection experinces.

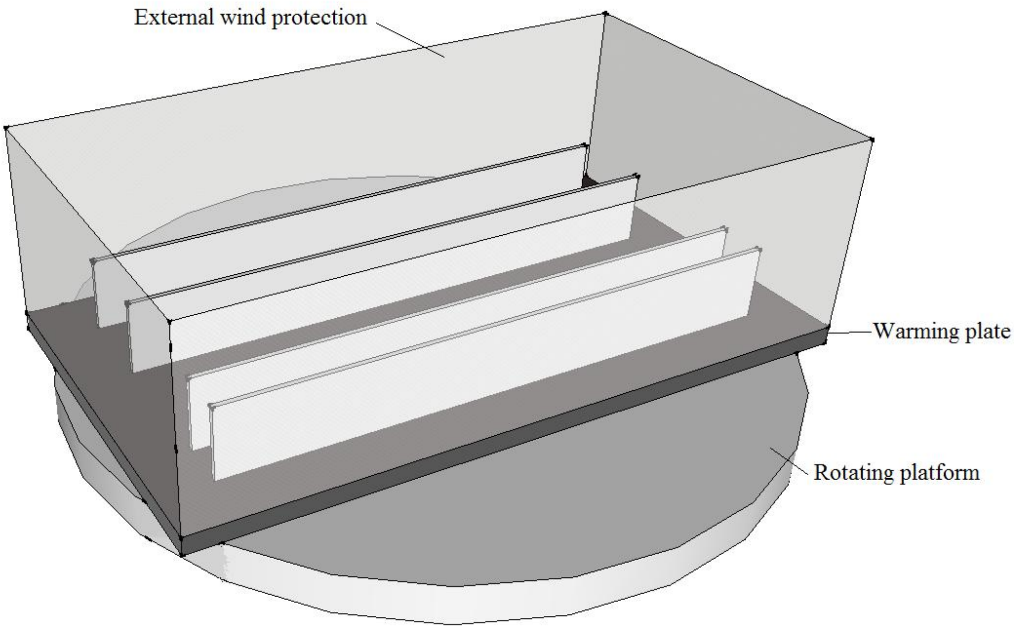

Figure **4:** Adaptation of the EF to the natural convection conditions

Forced convection

In the case of forced convection, h_c is given by:

$$hc = Nu \cdot \frac{\lambda}{l} \quad (16)$$

$$Nu = C \cdot Re^m \cdot Pr^n \quad (17)$$

$$Pr = \mu \cdot \frac{Cp}{k} \quad (18)$$

$$Re = \frac{\rho \cdot u \cdot L}{\mu} \quad (19)$$

where *Nu* is the Nusselt number, *Pr* is the Prandtl number, and *Re* Reynolds number with their usual definitions [24].

Since in eq. (19) the term $B = \frac{\rho}{\mu}$ is only dependent on the specific properties of the fluid participating to the convective heat transfer, it is univocally calculated. Therefore, the Reynolds number can be expressed by:

$$Re = B \cdot (u \cdot L) \quad (20)$$

The EF and the real scenario are connected by the following analogy relation:

$$u \cdot L = u_M \cdot L_M \quad (21)$$

The EF dimension (L_M) may be set forcing the longitudinal air velocity (u_M) (e.g. using a fan): For example, considering u=5 m/s and u_M=50 m/s, the scale ratio is L_M/L=0.1:

$$L_M = \frac{u}{u_M} \cdot L \quad (22)$$

The condition given in eq. (22) may be achieved making adjustments on the EF, that are:

- to use a protection barrier from the external wind without modifying the insolation;
- to install a fan producing an air flow in the longitudinal direction of each canyon; the air flow will be laminated prior entering each canyon.

In addition, the next configuration of the EF will include a particular rotating platform enabling to follow the Sun-path.

Figure 5 shows the EF configured for forced convection conditions.

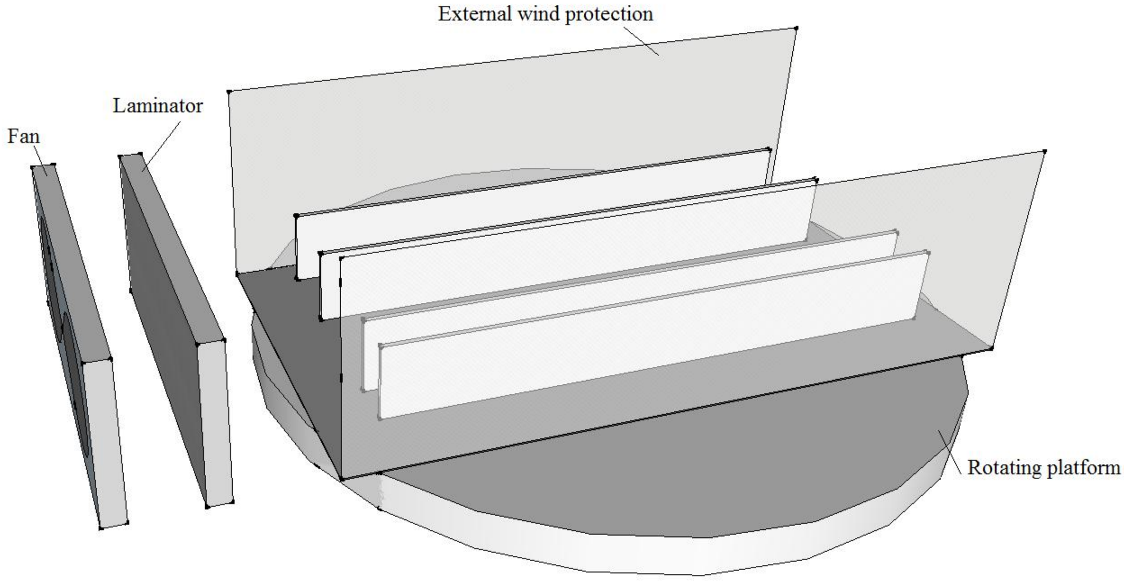

Figure **5:** Adaptation of the EF to the forced convection conditions.

4 TM VALIDATION AND BASELINE ANALYSIS

EF may be used directly to estimate UHI by a mechanical analogy which however introduces strong limitation on real scenario dimensions and operative conditions.
By validating the TM via EF the range of real scenario may be studied and predicted is widely extended and the proposed method may be applied virtually for any case.
The TM validation via EF may be done without using analogy relations; it will be carried out comparing the experimental results and the predicted values using appropriate geometric, radiative, and convective parameters.
Figure 6 provides a logical pattern between the real scenario, the EF, and the TM.

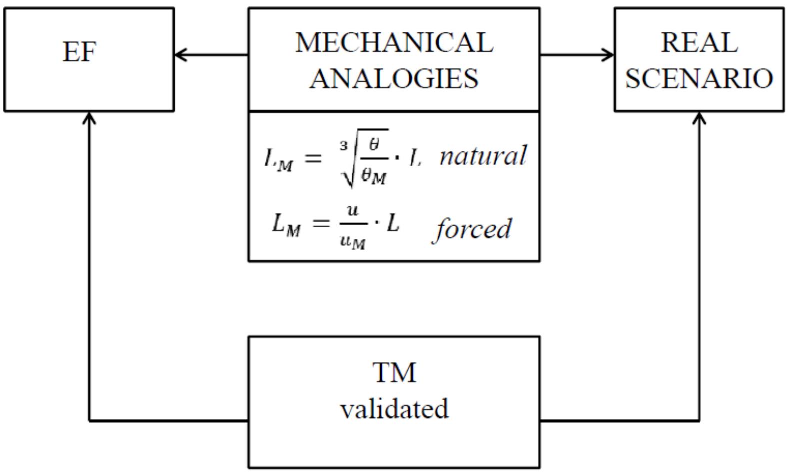

Figure 6: Logical pattern between the real scenario, the EF, and the validated TM.

The analysis of the surface properties bases on the difference observed the two test fields when the vertical surfaces have different reflective properties (e.g. to test the cooling performances of highly-reflective “cool” coverings). In an ideal case, i.e. identical canyons on both sides instrumented with equal-response sensors, each difference in the characteristic temperature can be attributed to the surface property change alone. In the real case, it is necessary to perform a baseline analysis to estimate the sensitivity of the EF to the specific parameter.

A preliminary calibration campaign was run from July 24th to July 29th 2013. Both of the test fields were South oriented and equipped with the same surface finishing (i.e. white extruded polystyrene) and instrumented with a limited number of sensors positioned at specular positions (i.e. at each West sensor corresponds the mirror East sensor). Ground and vertical surface temperatures and solar radiation were measured every 10 mins.

The result of the baseline shows that the average difference between mirror sensors is 0.45°C for the entire dataset and 0.05°C considering night-time data only. The slightly larger daylight difference suggests that the difference is attributable either to reflectivity or geometric differences between the two test fields. The average standard deviation is 0.77°C. This value represents the estimation of the sensitivity of the EF to a change of the reflective properties of the surfaces. This value of standard deviation is expected to be at about one order of magnitude lower than the temperature difference produced by the reflective films applied on the two mirror setup facilities. First results from the monitored data, carried out during the first week of August 2013, confirm this expectation. The maximum ground temperature (r = 7.5 %) is between 60 and 75°C, depending on the sensor position, produced with a maximum solar radiation of 1014 W/m^2.

5 CONCLUSIONS AND FUTURE DEVELOPMENT

A comprehensive approach to the Urban Heat Island effect, including analytical modelling and experimental measurements, is presented.

As a first result, an energy-balance analytic model (TM), predicting the behavior of a urban heat canyon as a function of meteorological conditions, geometry, and surface reflective properties was elaborated. The TM bases on a set of 10 equations taking into account separately visible and infrared radiosities and the total energy balance on each of the canyon surface. The system is fully determined (it involves a total of 10 variables), and returns the characteristic canyon temperatures for different boundary conditions.

As a second result, an EF was designed, implemented, and instrumented to resemble typical urban canyon conditions. The EF is composed of two twin test fields with adjustable height/distance ratios and interchangeable surface coverings. A total of 58 temperature sensors, a pyranometer and an anemometer were deployed.

In the first data taking period (July 24th to July 29th) the system stability was tested and an estimation of the sensitivity to the change of surface reflective properties was performed. The two test fields were equipped with the same covering and same geometry. Temperature measurements from specular sensor couple show an overall stability over the time, with an averaged standard deviation of 0.77°C. This result defines the sensitivity of the EF when comparing the performances of different-reflectivity coverings applied on equal-geometry urban canyons. First results confirm that this sensitivity value is less than one order of magnitude with respect to the expected difference produced by the application of films with different reflectance capability in the two parallel test facilities (EF), as carried during the first week of August 2013.

An intensive data-taking campaign is currently on-going. On each test field, the vertical surfaces of the canyons have the same reflective properties (high reflectivity on one side and low reflectivity on the other side). The results will be used to relate the reflectivity to the canyon characteristic temperature change. Measured wind speed will be included to correctly account for the convection heat transfer. A wind protective barrier will be also arranged. As a final step, the data will be used to validate the TM.

6 REFERENCES

[1] Shahidan, M. F., Jones, P. J., Gwilliam, J., Salleh, E. (2012). An evaluation of outdoor and building environment cooling achieved through combination modification of trees with ground materials. *Building and Environment*, 58, 245-257.

[2] Manley, G. (1958). On the frequency of snowfall in metropolitan England. Quarterly *Journal of the Royal Meteorological Society*, 84, 70-72.

[3] Taha, H. (1997). Urban climates and heat islands: albedo, evapotranspiration, and anthropogenic heat, *Energy and Buildings*, 25, 99-103.

[4] Giridharan, R., Kolokotroni, M. (2009). Urban heat island characteristics in London during winter, *Solar Energy*, 83, 1668-1682

[5] Howard, L. (2012). *Climate of London Deduced from Meteorological Observations*, Harvey and Darton 3rd ed.

[6] Pisello, A.L., Cotana, F., Nicolini, A., Brinchi, L. (2013). Development of Clay Tile Coatings for Steep-Sloped Cool Roofs. *Energies*, 6, 3637-3653.

[7] Santamouris, M. (2007). Heat island research in Europe—the state of the art, *Advances Building Energy Research*, 1(1), 123-150.

[8] Synnefa, A., Saliari, M., Santamouris, M. (2012). Experimental and numerical assessment of the impact of increased roof reflectance on a school building in Athens, *Energy and Buildings*, 55, 7-15.

[9] Pisello, A. L., Rossi, F., Cotana, F. (2012). On the impact of cool roofs in Italian residential buildings: experimental assessment of summer and winter performance, ICHMT Digital library on line, DOI: 10.1615/ICHMT.2012.SEBUA-12.220.

[10] Kolokotsa, D., Diakaki, C., Papantoniou, S., Vlissidis, A. (2012). Numerical and experimental analysis of cool roofs application on a laboratory building in Iraklion, Crete, Greece, *Energy and Buildings*, 55, 85-93

[11] Xu, X., Taylor, J.E., Pisello, A.L., Culligan, P. (2012). The impact of place-based affiliation networks on energy conservation: An holistic model that integrates the influence of buildings, residents and the neighborhood context, Energy and Buildings, 55, 637-646.

[12] Akbari, H., Matthews, D. H. (2012). Global cooling updates: Reflective roofs and pavements, Energy and Buildings, 55, , pp. 2-6.

[13] Gobakis, K., Kolokotsa, D., Synnefa, A., Saliari, M., Giannopoulou, K., Santamouris, M. (2011). Development of a model for urban heat island prediction using neural network techniques, *Sustainable Cities and Society*, 1, 104-115.

[14] Allegrini, J., Dorera, V., Carmelieta, J. (2012). Influence of the urban microclimate in street canyons on the energy demand for space cooling and heating of buildings, *Energy and Buildings*, 55, 823-832.

[15] Strømann-Andersen, J., Sattrup, P.A. (2011). The urban canyon and building energy use: Urban density versus daylight and passive solar gains, *Energy and Buildings*, 43, 2011-2020.

[16] Doya, M., Bozonnet, E., Allard, F. (2012). Experimental measurement of cool facades' performance in a dense urban environment, *Energy and Buildings*, 55, 42-50.

[17] Chan, A. T., So, E. S. P., Samad, S. C. (2001). Strategic guidelines for street canyon geometry to achieve sustainable street air quality, *Atmospheric Environment*, 35, 4089-4098.

[18] Krüger , E., Pearlmutter, D., Rasia, F. (2010). Evaluating the impact of canyon geometry and orientation on cooling loads in a high-mass building in a hot dry environment, *Applied Energy*, 87, 2068-2078.

[19] Bonacquisti, V., Casale, G.R., Palmieri, S., Siani, A.M. (2006). A canopy layer model and its application to Rome, *Science of the Total Environment*, 364,1-13.

[20] Ratti, C., Baker, N., Steemers, K. (2005). Energy consumption and urban texture, *Energy and Buildings*, 37, 762-776.

[21] ASTM International. Standard test method for solar absorptance, reflectance, and transmittance of materials using integrating spheres. 2012, ASTM 903-12, DOI: 10.1520/E0903-12.

[22] European Committee for Standardization. Glass in building – determination of luminous and solar characteristics of glazing. 2011, UNI EN 410:2011.

[23] M. Felli and C. Buratti. Lezioni di Fisica Tecnica 2. 2004. ISBN 88-89422-14-9.

[24] Y.A. Cengel, Termodinamica e trasmissione del calore, ed. McGraw-Hill, 1998.